

1 **Efficient *in planta* detection and dissection of *de novo* mutation events in the *Arabidopsis***
2 ***thaliana* disease resistance gene *UNI***

3

4 **Running head:** *In planta* dissection of mutation events in *UNI*

5

6 **Corresponding authors:**

7 **Masao Tasaka**

8 Graduate School of Biological Sciences, Nara Institute of Science and Technology, 8916-5
9 Takayama, Ikoma, 630-0192, Japan

10 Tel: (Japan: 81)-743-72-5480

11 E-mail: m-tasaka@bs.naist.jp

12

13 **Naoyuki Uchida**

14 Institute of Transformative Bio-Molecules (WPI-ITbM), Nagoya University, Furo-cho,
15 Chikusa-ku, Nagoya, 464-8601, Japan

16 Tel: (Japan: 81)-52-789-2841

17 E-mail: uchinao@itbm.nagoya-u.ac.jp

18

19 **Subject areas:** (2) environmental and stress responses, and (10) genomics, systems biology
20 and evolution

21

22 Black and white figures: 3, colour figures: 4, Tables: 0, Supplementary figures: 1,

23 Supplementary tables: 1

24 **Efficient *in planta* detection and dissection of *de novo* mutation events in the *Arabidopsis***
25 ***thaliana* disease resistance gene *UNI***

26

27 **Running head:** *In planta* dissection of mutation events in *UNI*

28

29 Tomohiko Ogawa^{1,4}, Akiko Mori^{2,4}, Kadunari Igari¹, Miyo Terao Morita², Masao Tasaka^{1,*}
30 and Naoyuki Uchida^{3,*}

31

32 ¹ Graduate School of Biological Sciences, Nara Institute of Science and Technology, 8916-5
33 Takayama, Ikoma, 630-0192, Japan

34 ² Graduate School of Bioagricultural Sciences, Nagoya University, Furo-cho, Chikusa-ku,
35 Nagoya, 464-8602, Japan

36 ³ Institute of Transformative Bio-Molecules (WPI-ITbM), Nagoya University, Furo-cho,
37 Chikusa-ku, Nagoya, 464-8601, Japan

38

39 ⁴ These authors contributed equally to this work.

40

41 **Abbreviations:** ATM, ATAXIA TELANGIECTASIA MUTATED; ATR, ATAXIA
42 TELANGIECTASIA MUTATED- AND RAD3-RELATED; Col, Columbia; DSB, double
43 strand break; EMS, ethyl methanesulfonate; HU, hydroxyurea; NB-LRR, nucleotide-binding
44 and leucine-rich-repeat; SA, salicylic acid; SNP, single-nucleotide polymorphism; Ws,
45 Wassilewskija

46 **Abstract**

47 Plants possess disease resistance (R) proteins encoded by *R* genes, and each R protein
48 recognizes a specific pathogen factor(s) for immunity. Interestingly, a remarkably high degree
49 of polymorphisms in *R* genes, which are traces of past mutation events during evolution,
50 suggest the rapid diversification of *R* genes. However, little is known about molecular aspects
51 that facilitate the rapid change of *R* genes because of the lack of tools that enable us to
52 efficiently monitor *de novo* *R* gene mutations in an experimentally feasible timescale,
53 especially in living plants. Here we introduce a model assay system that enables efficient *in*
54 *planta* detection of *de novo* mutation events in the *Arabidopsis thaliana* *R* gene *UNI* in one
55 generation. The *uni-1D* mutant harbors a gain-of-function allele of the *UNI* gene. *uni-1D*
56 heterozygous individuals originally exhibit dwarfism with abnormally short stems. However,
57 interestingly, morphologically normal stems sometimes emerge spontaneously from the
58 *uni-1D* plants, and the morphologically reverted tissues carry additional *de novo* mutations in
59 the *UNI* gene. Strikingly, under an extreme condition, almost half of the examined population
60 shows the reversion phenomenon. By taking advantage of this phenomenon, we demonstrate
61 that the reversion frequency is remarkably sensitive to a variety of fluctuations in DNA
62 stability, underlying a mutable tendency of the *UNI* gene. We also reveal that activities of
63 salicylic acid pathway and DNA damage sensor pathway are involved in the reversion
64 phenomenon. Thus, we provide an experimentally feasible model tool to explore factors and
65 conditions that significantly affect the *R* gene mutation phenomenon.

66

67 **Keywords:** *Arabidopsis thaliana*; DNA damage sensor pathway; *R* gene; mutation; Salicylic
68 acid pathway; *UNI*

69 **Introduction**

70 Because plants do not possess an adaptive immune system like that found in
71 vertebrates, they depend on an innate immune system. To induce strong immune responses in
72 this system, plants use disease resistance (R) proteins, which are encoded by *R* genes. Each R
73 protein serves as a sensor to recognize a specific pathogen factor(s) and triggers strong
74 immune responses (Heidrich et al. 2012; Takken and Goverse 2012). However, plants possess
75 only a limited number of *R* genes. For example, the reference accession of *Arabidopsis*
76 *thaliana*, Col-0, has only about 150 *R* genes (Meyers et al. 2003). On the other hand,
77 pathogen factors tend to evolve rapidly. This suggests that plants might not be able to respond
78 to an infinite number of newly emerging pathogen factors just by utilizing the existing *R*
79 genes though the “guard hypothesis” proposes that some R proteins are able to indirectly
80 recognize pathogen infection by sensing changes in plant proteins targeted by pathogen
81 factors (Dangl and Jones 2001). Thus, *R* genes are also required to rapidly evolve to counter
82 the rapid diversification of pathogen factors, and actually a high degree of polymorphisms are
83 observed in *R* genes among species or intraspecific accessions, implicating the rapid evolution
84 of *R* genes (Anderson et al. 2010; Cao et al. 2011; Gan et al. 2011; Guo et al. 2011). However,
85 little is known about mechanisms underlying their rapid evolution because of the lack of tools
86 to efficiently detect *de novo* nucleotide changes in *R* genes in an experimentally feasible
87 timescale.

88 Interestingly, an increasing number of *R* genes have been highlighted as responsible
89 loci for hybrid incompatibility (Alcazar et al. 2009; Bomblies et al. 2007; Chae et al. 2014;
90 Phadnis and Malik 2014). Incompatible gene combinations in F1 hybrids cause inappropriate
91 activation of immune responses that leads to growth inhibition (Bomblies and Weigel 2007).

92 Because the hybrid incompatibility is one of major gene-flow barriers between species and
93 thus affects speciation, the *R* gene diversification has been recognized as an important factor
94 that may contribute to the evolution of plants (Bomblies and Weigel 2007). Therefore, the
95 elucidation of molecular mechanisms for *R* gene diversification would provide novel insights
96 into driving forces for the plant evolution.

97 Here we introduce a novel model system that enables us to efficiently and
98 practically detect *R* gene mutation events in living plants in one generation. The *Arabidopsis*
99 *thaliana* mutant *uni-ID* originally exhibits dwarfism due to a gain-of-function mutation in the
100 *UNI* gene, an *R* gene (Igari et al. 2008). Interestingly, in this mutant, morphological reversion
101 that is accompanied by *de novo* mutations in the *UNI* gene frequently occurs. By taking
102 advantage of this phenomenon, we demonstrate that the reversion phenomenon is remarkably
103 sensitive to a variety of conditions that affect DNA stability, implicating a mutable tendency
104 of the *UNI* gene as an *R* gene. We also show that salicylic acid (SA) pathway, which R
105 proteins activates for immunity, and DNA damage sensor pathway are involved in the
106 reversion event. Thus, we provide a practical model tool to explore factors and conditions that
107 significantly affect the *R* gene mutation phenomenon.

108 **Results**

109

110 **An additional mutation that occurs in the *UNI-ID* gene is visually detected as a**
111 **morphological reverted stem.**

112 The *Arabidopsis thaliana* mutant *uni-ID* carries a semi-dominant allele of the *UNI*
113 gene (Igari et al. 2008), which is a typical *R* gene encoding an NB-LRR (nucleotide-binding
114 and leucine-rich-repeat)-type R protein. Because the *uni-ID* mutation converts UNI proteins
115 into an active form, *uni-ID* plants constitutively exhibit some immune responses even without
116 any pathogen infection. Due to the severe immune responses, *uni-ID* homozygous plants stop
117 growing at a seedling stage. On the other hand, *uni-ID* heterozygous plants (hereafter
118 *uni-ID/+*) are fertile, though they display severe dwarfism and produce remarkably short
119 stems (Fig. 1A, left). Interestingly, we repeatedly observed that, under normal growth
120 condition, *uni-ID/+* plants sometimes produced wild-type-like long stems spontaneously (Fig.
121 1A, right). When the *UNI-ID* gene in the morphologically reverted stem was sequenced in
122 each case, an additional *de novo* intragenic mutation was identified in the *UNI-ID* gene (Fig.
123 1B). This observation could be explained as follows (Fig. 1C); a *de novo* intragenic
124 loss-of-function mutation that attenuates the UNI-ID protein activity is generated in the
125 *uni-ID* gene in one cell at a leaf axil where axillary stems are generally formed. The mutated
126 cell proliferates as normal as a wild-type cell because the mutated cell is released from the
127 cellular growth defect induced by the original *uni-ID* mutation. Then, the sector consisting of
128 the proliferating mutated cells eventually gives rise to a morphologically reverted
129 wild-type-like stem. Therefore, an additional intragenic mutation is detected in the reverted
130 stem. Since mutation events in the *uni-ID* gene are easily detected as morphological

131 reversions in *uni-ID/+* plants, we expected that this phenomenon could be utilized as a model
132 assay system to experimentally explore molecular aspects for the diversification of *R* genes,
133 which had not been achieved so far due to the lack of tools to efficiently detect *de novo*
134 nucleotide changes in *R* genes in living plants.

135

136 **The frequency of the *UNI-ID* reversion is remarkably enhanced by EMS treatment.**

137 At first, to develop this assay system to more efficient one, we aimed to increase
138 reversion frequency in *uni-ID/+* plants. To that end, *uni-ID/+* plants were treated with ethyl
139 methanesulfonate (EMS), an alkylating agent that mainly induces point mutations by directly
140 attacking DNAs. As the EMS concentration increased, reversion efficiency drastically
141 increased (Fig. 2A), while too high concentration of EMS 1% severely affected germination
142 rate (Fig. 2A). As shown in Supplementary Fig. 1, the highest reversion frequency was
143 observed when *uni-ID/+* plants were treated with 0.3% EMS for 27 hours. Strikingly, under
144 this condition, almost half of germinated *uni-ID/+* population showed reversion phenomenon,
145 likely representing a mutable tendency of *R* genes, though half of the EMS-treated seeds did
146 not germinate. By considering the balance between reversion frequency and germination rate,
147 the treatment of 0.3% EMS for 15 hours (Fig. 2A) was chosen to facilitate reversion
148 phenomenon for most of later experiments. To verify an association between the
149 EMS-induced morphological reversion and the introduction of additional *de novo* intragenic
150 mutations in the *UNI-ID* gene, the *UNI-ID* gene derived from the morphologically reverted
151 stems was sequenced using randomly picked-up samples. As a result, additional mutations
152 were identified in all the cases examined (Fig. 2B) and they were all canonical EMS-type
153 G:C-to-A:T nucleotide substitutions, strongly suggesting that the morphological reversion

154 was caused by EMS-induced intragenic mutations within the *UNI-ID* gene.

155

156 **The high frequency of the *UNI-ID* reversion does not depend on the original cluster**
157 **structure surrounding the *UNI* locus**

158 The *UNI* gene and its homologous genes are located as a gene cluster in the
159 *Arabidopsis thaliana* genome (Igari et al. 2008) (Fig. 3A). Most *R* genes reside in clusters and
160 the clustered arrangement has been considered as one of driving forces of *R* gene evolution
161 via recombination or gene conversion (Ameline-Torregrosa et al. 2008; Guo et al. 2011; Luo
162 et al. 2012; Meyers et al. 2003; Richly et al. 2002; Shao et al. 2014). To examine whether the
163 cluster structure surrounding the *UNI* locus is necessary for the frequent reversion observed in
164 the *uni-ID/+* plants (Fig. 2), we analyzed reversion frequency in transgenic plants that
165 reproduced the *uni-ID/+* phenotype by the introduction of the 5.3-kb genomic fragment
166 containing only the *uni-ID* gene into the wild-type background. When the plants
167 hemizygotously carrying the *uni-ID* transgene (hereafter *uni-ID^{Tr}+* plants) were treated with
168 EMS, 28% of the treated individuals exhibited morphological reversion (Fig. 3B), which was
169 comparable to the case of the original *uni-ID/+* plants. This indicates that the 5.3-kb *uni-ID*
170 transgene which does not contain the original gene cluster structure was sufficient for the
171 reversion phenomenon. Furthermore, the *uni-ID* mutant was originally isolated in Ws
172 background. To examine whether the original background was required for the frequent
173 reversion, we analyzed reversion frequency in the introgression line harboring the *uni-ID*
174 allele in Col background. When the *uni-ID/+* (Col) plants were treated with EMS, the
175 reversion was observed as frequently as in the case of the original *uni-ID/+* (Ws) (Fig. 3B),
176 showing that the frequent reversion was not specific to the Ws background.

177

178 **The *UNI-ID* reversion phenomenon is sensitive to various types of fluctuations in DNA**
179 **stability.**

180 To examine whether the *uni-ID*-based assay system can be applied to detection of
181 various types of fluctuations in DNA stability, *uni-ID/+* plants were exposed to conditions
182 that affect DNA stability other than EMS treatment. When *uni-ID/+* plants were treated with
183 the radiomimetic drug Zeocin that induces double strand breaks (DSBs) of DNA, reversion
184 frequency significantly increased (Fig. 4A). Then the *UNI-ID* gene in the reverted stems was
185 sequenced to check *de novo* intragenic mutations were induced. In contrast to the EMS
186 treatment that induced point mutations (Fig. 2), the Zeocin treatment caused deletion
187 mutations varying in size from 1 bp to 43 bp (Fig. 4B, upper side), which was consistent with
188 previous reports that DSBs often produced deletion mutations via error-prone nonhomologous
189 end-joining DNA repair pathway (Hyun et al. 2014; Jiang et al. 2014; Jiang et al. 2013; Knoll
190 et al. 2014; Lloyd et al. 2012). Next, *uni-ID/+* plants were treated with hydroxyurea (HU)
191 that is used to mimic replication blocks caused by UV- or gamma radiation-induced DNA
192 damage (Biever et al. 2014; Culligan et al. 2004; Roa et al. 2009). HU also increased
193 reversion frequency (Fig. 4A). In this case, identified *de novo* intragenic mutations in the
194 *UNI-ID* gene were point mutations (Fig. 4B, lower side). In contrast to the EMS treatment
195 that specifically produced G:C-to-A:T transitions (Fig. 2), the HU-induced nucleotide
196 substitutions appeared random. This observation is reasonable because EMS particularly
197 produces guanine alkylation resulting in canonical G:C-to-A:T transitions, while HU does not
198 specify particular types of nucleotide changes as it indirectly causes DNA damage through its
199 replication blocking activity. The above results indicated that this assay system could be used

200 to examine what conditions or what type of fluctuations in DNA stability affect the stability
201 of the *UNI-ID* gene. Therefore, by taking advantage of this *UNI-ID*-based system, we next
202 explored molecular aspects that could be involved in *R* gene diversification.

203

204 **The activation of salicylic acid pathway enhances the *UNI-ID* reversion phenomenon.**

205 It was previously reported that pathogen infection increases the frequency of
206 somatic homologous recombination (Kovalchuk et al. 2003; Yao et al. 2011). Though
207 beta-glucuronidase- or luciferase-based reporter genes were used to detect somatic
208 recombinations in these studies (Kovalchuk et al. 1998; Kovalchuk et al. 2003), we
209 hypothesized that some pathogenesis-related responses might affect not only the stability of
210 these reporter transgenes but also that of some endogenous genes including *R* genes.
211 Meanwhile, salicylic acid (SA) pathway, one of major pathogenesis-related responses, is
212 activated in *uni-ID/+* (Igari et al. 2008). Thus, the possibility was raised that activation of the
213 SA pathway might be involved in fluctuations of *R* gene stability. To examine this possibility,
214 *sid2 uni-ID/+* double mutant plants, in which the SA pathway is inactivated due to the loss of
215 the gene critical for SA biosynthesis, were treated with EMS, and then reversion frequency
216 was analyzed. As shown in Fig. 5, the reversion frequency in *sid2 uni-ID/+* was about as half
217 as that in *uni-ID/+*, indicating that reversion was promoted by activation of SA pathway.
218 However, since the reversion phenomenon was not completely suppressed by inactivation of
219 the SA pathway, other mechanisms activated by the R protein signaling may also be involved
220 in the regulation of the *R* gene stability.

221

222 ***ATR*, a component of the DNA damage sensor system, is involved in the *UNI-ID***

223 **reversion phenomenon.**

224 Recently it was reported that a component of DNA damage sensor system, ATR
225 (ATAXIA TELANGIECTASIA MUTATED- AND RAD3-RELATED), was involved in
226 plant immune responses, indicating a link between immune responses and the DNA damage
227 signaling (Yan et al. 2013). As the SA pathway, which is one of immune signaling pathways,
228 was involved in the reversion phenomenon in *uni-ID/+* (Fig. 5), we examined whether *ATR*
229 or its close relative gene *ATM* (ATAXIA TELANGIECTASIA MUTATED) might also
230 contribute to this phenomenon. As shown in Fig. 6, even under the normal condition without
231 any treatment, the reversion frequency in *atr uni-ID/+* was higher than that in *uni-ID/+*. On
232 the other hand, reversion was not accelerated in *atm uni-ID/+*. Next, *uni-ID/+*, *atr uni-ID/+*
233 and *atm uni-ID/+* were treated with a low concentration (0.1%) of EMS. The reversion
234 frequency in *atm uni-ID/+* was comparable to that of *uni-ID/+*, while *atr uni-ID/+* displayed
235 a significantly higher reversion frequency than *uni-ID/+* and *atm uni-ID/+*. These data
236 indicated that *ATR*, but not *ATM*, was involved in the regulation of the *R* gene stability. This
237 may be related to the previous reports that *ATR* and *ATM* play distinct roles in DNA damage
238 sensor system (Culligan et al. 2004) and that *ATR* links the DNA damage signaling with
239 immune responses but *ATM* does not (Yan et al. 2013).

240

241 **Biased production of *de novo* SNPs at the whole genome level is not observed in *uni-ID/+***
242 **plants.**

243 Our findings described above show that nucleotide changes in the *UNI-ID* gene are
244 frequently observed in *uni-ID/+* plants. To examine whether stability of other genomic
245 regions are also affected in *uni-ID/+*, spectrum of *de novo* spontaneous single-nucleotide

246 polymorphisms (SNPs) generated in wild-type and *uni-ID^{T/+}* plants in the uniform
247 background (Fig. 7A) was genome-widely analyzed by the single-seed-descent-based method
248 (Ossowski et al. 2010). As shown in Fig. 7 and Table S1, no obvious difference was observed
249 between wild type and *uni-ID^{T/+}* in terms of the number of detected *de novo* SNPs (Fig. 7B),
250 the spectrum of their nucleotide substitutions (Fig. 7C) and the categorization of the detected
251 SNPs according to genic characters (Fig. 7D), suggesting that *uni-ID^{T/+}* might not make a
252 detectable impact on nucleotide stability at the whole genome level, at least in a manner that
253 could be examined by this approach.

254 **Discussion**

255 In this work, we introduced the assay system that efficiently detects *de novo*
256 mutation events in the *UNI-ID* gene as a morphological reversion. Strikingly, in the most
257 extreme case as shown in Supplementary Fig. 1, almost half of the examined population
258 showed the reversion phenomenon, which likely reflects a mutable tendency of the *UNI* gene
259 as an *R* gene. Considering what mechanisms could increase mutation frequency of specific
260 genes like *R* genes, it would be rational to divide the mutation phenomenon into the following
261 three levels; (1) molecules that directly attack the DNA, (2) the protection of DNAs from the
262 attacking molecules and (3) the repair of the damaged DNA. Among these, it is unlikely that
263 attacking molecules such as natural or artificial mutagens (ultraviolet radiation, alkylating
264 agents, double strand break inducers, reactive oxygen species and so on) selectively interact
265 with specific genes. On the other hand, the selective protection of specific genes from
266 attacking molecules may be possible. Differences in chromatin structures like tightly packed
267 heterochromatin regions or open euchromatin regions may affect the accessibility of attacking
268 molecules to specific genes. In this viewpoint, gene- or region-specific DNA and/or histone
269 modifications that induce changes of chromatin structures could be important for the
270 modulation of the accessibility of attacking molecules. Though it is unknown whether specific
271 chromatin modifications are observed at *R* gene loci, it was reported that some *R* gene loci are
272 regulated by small RNAs (Marone et al. 2013; Park and Shin 2015; Yi and Richards 2007).
273 Since small RNAs often induce changes in chromatin situations of their target genes (Holoch
274 and Moazed 2015; Matzke and Mosher 2014; Saze et al. 2012; Simon and Meyers 2011), the
275 selective changes of chromatin modifications in specific *R* genes could be achieved mediated
276 through small RNAs. Similarly, the selective exclusion of DNA repair machinery from

277 specific *R* genes to induce frequent mutations may also be possible via small RNAs because
278 recent studies have shown the existence of small RNA-directed repair of damaged DNAs
279 (Gao et al. 2014; Oliver et al. 2014; Wei et al. 2012; Yang and Qi 2015). Thus, detailed
280 analysis on relationships between the *UNI* gene, small RNA species and chromatin conditions
281 might provide further insight into the mechanisms that increase the mutation frequency of the
282 *UNI* gene.

283 The high rate of recombination or gene conversion among the *R* genes which form a
284 cluster structure is recognized as one of major forces that lead to the rapid evolution of the *R*
285 genes (Ellis et al. 2000; Friedman and Baker 2007; Joshi and Nayak 2013; McDowell and
286 Simon 2006). However, though the *UNI* gene and its homologous genes form a gene cluster
287 (Fig. 3), mutations caused by recombination or gene conversion have not been detected so far
288 in our experiments. The rate of recombination or gene conversion events may not be higher in
289 the *UNI* locus than in general genes. This observation may be related with the fact that the
290 frequent reversion phenomenon in *uni-1D/+* plants does not depend on the cluster structure
291 surrounding the *UNI* locus (Fig. 3). Another characteristic of the *uni-1D*-based assay is that it
292 detects only loss-of-function mutations which attenuate the activity of UNI-1D proteins (Fig.
293 1C). Therefore, the actual mutation frequency that reflects any type of mutations including
294 silent ones would be much higher. In addition, in the *uni-1D*-based assay, the mutations need
295 to occur in cells that possess an ability to give rise to stems (Fig. 1C). If a methodology that
296 overcomes these limitations be established, it would facilitate further understanding of
297 molecular aspects underlying the *UNI* gene diversification. The genome-wide SNP analysis
298 by the single-seed-descent-based method (Fig. 7A) did not detect obvious differences
299 between wild type and *uni-1D/+* (Fig. 7B-D). This result may be due to the bias of cells

300 targeted by this method because it detects only *de novo* SNPs that are eventually inherited to
301 one fertilized egg cell in each generation. If a methodology be developed by which *de novo*
302 SNPs in any cell of the plant body are genome-widely detected, some differences might be
303 observed between wild type and *uni-ID/+*.

304 As shown in Fig. 5, reversion phenomenon in *uni-ID/+* was promoted by activation
305 of the SA pathway that is one of major immune responses. However, since the reversion was
306 not completely suppressed by inactivation of the SA pathway (Fig. 5), other immune-related
307 pathways activated by UNI-1D proteins may also be involved in the reversion phenomenon.
308 An important question to be addressed in the future is whether the activation of such immune
309 responses including the SA pathway are necessary for rapid diversification of the wild-type
310 *UNI* gene and also other *R* genes in wild-type background. To address this question, instead
311 of the *uni-ID*-based assay system that only detects mutations of the *UNI-ID* gene in the
312 *uni-ID* background, a novel methodology that makes it possible to analyze mutation
313 frequency of various *R* genes including the *UNI* gene in wild-type background in an
314 experimentally feasible timescale would need to be developed. The similar issue may be
315 raised regarding the involvement of *ATR*. Though our data show that the loss of *ATR*
316 significantly enhances mutation frequency of the *UNI-ID* gene in the *uni-ID* background (Fig.
317 6), it is still unknown whether and how stability of the wild-type *UNI* gene is altered in the *atr*
318 single mutant background that does not harbor the *uni-ID* allele. To address this issue, the
319 above-mentioned methodology to analyze mutation frequency in non-*uni-ID* backgrounds
320 would be required for future studies.

321 In this work, we showed that *uni-ID/+* could be utilized as an experimentally
322 feasible tool to explore molecular aspects for the diversification of the *UNI-ID* gene. One of

323 important challenges would be to investigate whether the findings revealed by this tool can be
324 applicable to stability control of any *R* gene or specific *R* genes. It was previously reported
325 that phenotypes caused by duplication of the *Arabidopsis thaliana* *RPP5* *R*-gene cluster,
326 which includes seven *R* genes, was also frequently suppressed by EMS treatment (Yi and
327 Richards 2007, 2008) and, among such suppressor lines, three mutations have been identified
328 in one of the clustered *R* genes, *SNCI* (Yi and Richards 2009). It is interesting to examine
329 whether the factors revealed by the *UNI-ID*-based system, in which the *R*-gene cluster
330 structure around the *UNI* locus is not required for frequent mutations (Fig. 3), may be
331 commonly involved in the mutation phenomenon at the *RPP5* *R*-gene cluster locus. Another
332 practical use of this tool is to collect information about amino-acid residues that are important
333 for *R* protein activity since it is easy to identify a remarkably large number of such residues
334 by this tool (Fig. 2B). This information would facilitate the structural understanding of *R*
335 proteins. Interestingly, an increasing number of *R* genes have been recently highlighted also
336 as responsible loci for hybrid incompatibility (Alcazar et al. 2009; Bomblies et al. 2007;
337 Bomblies and Weigel 2007; Chae et al. 2014; Phadnis and Malik 2014), which is one of
338 major gene-flow barriers between species (Bomblies and Weigel 2007). Thus, the insight
339 provided by this study and future related studies would contribute to understanding of
340 molecular aspects that affect not only the *R* gene diversification but also even speciation.

341 **Materials and Methods**

342

343 **Plant materials, chemical treatments and growth conditions**

344 Plants were grown at 22°C under continuous light. *atr* and *atm* mutants in the Ws background
345 are FLAG_157C07 and FLAG_398A06 lines, respectively. To make *uni-ID^{T/+}* (Ws) and
346 *uni-ID^{T/+}* (Col), the previously reported *uni-ID* genomic fragment (Igari et al. 2008) was
347 introduced into Col or Ws plants. In EMS treatment assays, *uni-ID/+* seeds were treated with
348 indicated concentrations of EMS for 15 or 27 hours, washed thoroughly by water and then
349 germinated on MS agar plates. After 2 weeks after germination, *uni-ID/+* seedlings were
350 selected by their morphological phenotypes and transferred to soil. For Zeocin or HU
351 treatments, seeds were germinated and grown on MS agar plates containing 10 µg/l Zeocin or
352 1 mM HU. After 3 weeks after germination, *uni-ID/+* plants were transferred to soil. 50–100
353 plants were analyzed in each experiment to examine the frequency of morphological reversion
354 events.

355

356 **Sequencing of the *uni-ID* gene**

357 The *uni-ID* fragment covering the entire ORF was first amplified by either of the following
358 primer sets: for endogenous *uni-ID* gene, TCG ACA TCT CAC GCA TTG TTG and GAC
359 ACT GCA AGA TGA AAG AGA AAC; for transgenic *uni-ID* fragment, TCG ACA TCT
360 CAC GCA TTG TTG and AAG GGG GAT GTG CTG CAA GG. Then, the amplified
361 fragments were sequenced by the following primers: TGA GCT TCA AAA GTT GTG TC,
362 TGC TAG ATG ATA TGT GGG AG, ACT GGA TAT GCG AAG GAT TC, AAG AAT
363 AGA GCA ACT GCC TG, CAA AGA GAA AGC AAC CAA TC and ATG ATT CCG ACT

364 CCA TCT TC.

365

366 **Genome-wide analysis of *de novo* SNPs**

367 As shown in Fig. 7, *de novo* SNPs were analyzed using 4 independent lines per
368 genotype, which were all derived from a single Col-0 individual. To uniform backgrounds
369 between wild-type and *uni-ID* lines, the parental Col-0 line was transformed with the *uni-ID*
370 genomic fragment to generate *uni-ID* phenotypes. A single *uni-ID*^{T/+} plant was used as the
371 common parent of all *uni-ID*^{T/+} lines for later procedures. These lines were maintained by
372 selfing and single-seed descent during 5 generations. In the case of each *uni-ID*^{T/+} line, a
373 hemizygous *uni-ID*^{T/+} individual was selected by its morphological phenotype in each
374 generation. The plants after 5 generations were subjected to genome sequencing (Illumina
375 HiSeq 2000). 100-base single-end reads were mapped to the reference Col-0 genome
376 (TAIR10) by Strand NGS ver. 2.1 (Strand Scientific Intelligence Inc). *De novo* homozygous
377 SNPs were extracted according to the previously reported ‘consensus approach’ (Ossowski et
378 al. 2010).

379 **Funding**

380 This work was supported by MEXT/JSPS KAKENHI (Grant number 22657015 to M.T.;

381 Grant numbers 24113513 and 26113707 to N.U.).

382

383 **Disclosures**

384 The authors have no conflicts of interest to declare.

385 **References**

386

387 Alcazar, R., Garcia, A.V., Parker, J.E. and Reymond, M. (2009) Incremental steps toward
388 incompatibility revealed by Arabidopsis epistatic interactions modulating salicylic acid
389 pathway activation. *Proc. Natl. Acad. Sci. U. S. A.* 106: 334-339.

390

391 Ameline-Torregrosa, C., Wang, B.B., O'Bleness, M.S., Deshpande, S., Zhu, H., Roe, B., et al.
392 (2008) Identification and characterization of nucleotide-binding site-leucine-rich repeat genes
393 in the model plant *Medicago truncatula*. *Plant Physiol.* 146: 5-21.

394

395 Anderson, J.P., Gleason, C.A., Foley, R.C., Thrall, P.H., Burdon, J.B. and Singh, K.B. (2010)
396 Plants versus pathogens: an evolutionary arms race. *Funct. Plant Biol.* 37: 499-512.

397

398 Biever, J.J., Brinkman, D. and Gardner, G. (2014) UV-B inhibition of hypocotyl growth in
399 etiolated *Arabidopsis thaliana* seedlings is a consequence of cell cycle arrest initiated by
400 photodimer accumulation. *J. Exp. Bot.* 65: 2949-2961.

401

402 Bomblies, K., Lempe, J., Epple, P., Warthmann, N., Lanz, C., Dangl, J.L., et al. (2007)
403 Autoimmune response as a mechanism for a Dobzhansky-Muller-type incompatibility
404 syndrome in plants. *PLoS Biol.* 5: e236.

405

406 Bomblies, K. and Weigel, D. (2007) Hybrid necrosis: autoimmunity as a potential gene-flow
407 barrier in plant species. *Nat. Rev. Genet.* 8: 382-393.

408

409 Cao, J., Schneeberger, K., Ossowski, S., Gunther, T., Bender, S., Fitz, J., et al. (2011)
410 Whole-genome sequencing of multiple *Arabidopsis thaliana* populations. *Nat. Genet.* 43:
411 956-963.

412

413 Chae, E., Bomblies, K., Kim, S.T., Karelina, D., Zaidem, M., Ossowski, S., et al. (2014)
414 Species-wide genetic incompatibility analysis identifies immune genes as hot spots of
415 deleterious epistasis. *Cell* 159: 1341-1351.

416

417 Culligan, K., Tissier, A. and Britt, A. (2004) ATR regulates a G2-phase cell-cycle checkpoint
418 in *Arabidopsis thaliana*. *Plant Cell* 16: 1091-1104.

419

420 Dangl, J.L. and Jones, J.D. (2001) Plant pathogens and integrated defence responses to
421 infection. *Nature* 411:826-33.

422

423 Ellis, J., Dodds, P. and Pryor, T. (2000) Structure, function and evolution of plant disease
424 resistance genes. *Curr. Opin. Plant Biol.* 3: 278-284.

425

426 Friedman, A.R. and Baker, B.J. (2007) The evolution of resistance genes in multi-protein
427 plant resistance systems. *Curr. Opin. Genet. Dev.* 17: 493-499.

428

429 Gan, X., Stegle, O., Behr, J., Steffen, J.G., Drewe, P., Hildebrand, K.L., et al. (2011) Multiple
430 reference genomes and transcriptomes for *Arabidopsis thaliana*. *Nature* 477: 419-423.

431

432 Gao, M., Wei, W., Li, M.M., Wu, Y.S., Ba, Z., Jin, K.X., et al. (2014) Ago2 facilitates Rad51
433 recruitment and DNA double-strand break repair by homologous recombination. *Cell Res.* 24:
434 532-541.

435

436 Guo, Y.L., Fitz, J., Schneeberger, K., Ossowski, S., Cao, J. and Weigel, D. (2011)
437 Genome-wide comparison of nucleotide-binding site-leucine-rich repeat-encoding genes in
438 Arabidopsis. *Plant Physiol.* 157: 757-769.

439

440 Heidrich, K., Blanvillain-Baufume, S. and Parker, J.E. (2012) Molecular and spatial
441 constraints on NB-LRR receptor signaling. *Curr. Opin. Plant Biol.* 15: 385-391.

442

443 Holoch, D. and Moazed, D. (2015) RNA-mediated epigenetic regulation of gene expression.
444 *Nat. Rev. Genet.* 16: 71-84.

445

446 Hyun, Y., Kim, J., Cho, S.W., Choi, Y., Kim, J.S. and Coupland, G. (2014) Site-directed
447 mutagenesis in Arabidopsis thaliana using dividing tissue-targeted RGEN of the CRISPR/Cas
448 system to generate heritable null alleles. *Planta* 241: 271-284.

449

450 Igari, K., Endo, S., Hibara, K., Aida, M., Sakakibara, H., Kawasaki, T., et al. (2008)
451 Constitutive activation of a CC-NB-LRR protein alters morphogenesis through the cytokinin
452 pathway in Arabidopsis. *Plant J.* 55: 14-27.

453

454 Jiang, W., Yang, B. and Weeks, D.P. (2014) Efficient CRISPR/Cas9-mediated gene editing in
455 *Arabidopsis thaliana* and inheritance of modified genes in the T2 and T3 generations. *PLoS*
456 *One* 9: e99225.

457

458 Jiang, W., Zhou, H., Bi, H., Fromm, M., Yang, B. and Weeks, D.P. (2013) Demonstration of
459 CRISPR/Cas9/sgRNA-mediated targeted gene modification in *Arabidopsis*, tobacco, sorghum
460 and rice. *Nucleic Acids Res.* 41: e188.

461

462 Joshi, R.K. and Nayak, S. (2013) Perspectives of genomic diversification and molecular
463 recombination towards R-gene evolution in plants. *Physiol. Mol. Biol. Plants* 19: 1-9.

464

465 Knoll, A., Fauser, F. and Puchta, H. (2014) DNA recombination in somatic plant cells:
466 mechanisms and evolutionary consequences. *Chromosome Res.* 22: 191-201.

467

468 Kovalchuk, I., Kovalchuk, O., Arkhipov, A. and Hohn, B. (1998) Transgenic plants are
469 sensitive bioindicators of nuclear pollution caused by the Chernobyl accident. *Nat. Biotechnol.*
470 16: 1054-1059.

471

472 Kovalchuk, I., Kovalchuk, O., Kalck, V., Boyko, V., Filkowski, J., Heinlein, M., et al. (2003)
473 Pathogen-induced systemic plant signal triggers DNA rearrangements. *Nature* 423: 760-762.

474

475 Lloyd, A.H., Wang, D. and Timmis, J.N. (2012) Single molecule PCR reveals similar patterns
476 of non-homologous DSB repair in tobacco and *Arabidopsis*. *PLoS One* 7: e32255.

477

478 Luo, S., Zhang, Y., Hu, Q., Chen, J., Li, K., Lu, C., et al. (2012) Dynamic nucleotide-binding
479 site and leucine-rich repeat-encoding genes in the grass family. *Plant Physiol.* 159: 197-210.

480

481 Marone, D., Russo, M.A., Laido, G., De Leonardis, A.M. and Mastrangelo, A.M. (2013) Plant
482 nucleotide binding site-leucine-rich repeat (NBS-LRR) genes: active guardians in host
483 defense responses. *Int. J. Mol. Sci.* 14: 7302-7326.

484

485 Matzke, M.A. and Mosher, R.A. (2014) RNA-directed DNA methylation: an epigenetic
486 pathway of increasing complexity. *Nat. Rev. Genet.* 15: 394-408.

487

488 McDowell, J.M. and Simon, S.A. (2006) Recent insights into R gene evolution. *Mol. Plant*
489 *Pathol.* 7: 437-448.

490

491 Meyers, B.C., Kozik, A., Griego, A., Kuang, H. and Michelmore, R.W. (2003) Genome-wide
492 analysis of NBS-LRR-encoding genes in Arabidopsis. *Plant Cell* 15: 809-834.

493

494 Oliver, C., Santos, J.L. and Pradillo, M. (2014) On the role of some ARGONAUTE proteins
495 in meiosis and DNA repair in Arabidopsis thaliana. *Front. Plant Sci.* 5: 177.

496

497 Ossowski, S., Schneeberger, K., Lucas-Lledo, J.I., Warthmann, N., Clark, R.M., Shaw, R.G.,
498 et al. (2010) The rate and molecular spectrum of spontaneous mutations in Arabidopsis
499 thaliana. *Science* 327: 92-94.

500

501 Park, J.H. and Shin, C. (2015) The role of plant small RNAs in NB-LRR regulation. *Brief*
502 *Funct. Genomics* 14: 268-274.

503

504 Phadnis, N. and Malik, H.S. (2014) Speciation via autoimmunity: a dangerous mix. *Cell* 159:
505 1247-1249.

506

507 Richly, E., Kurth, J. and Leister, D. (2002) Mode of amplification and reorganization of
508 resistance genes during recent *Arabidopsis thaliana* evolution. *Mol. Biol. Evol.* 19: 76-84.

509

510 Roa, H., Lang, J., Culligan, K.M., Keller, M., Holec, S., Cognat, V., et al. (2009)
511 Ribonucleotide reductase regulation in response to genotoxic stress in *Arabidopsis*. *Plant*
512 *Physiol.* 151: 461-471.

513

514 Saze, H., Tsugane, K., Kanno, T. and Nishimura, T. (2012) DNA methylation in plants:
515 relationship to small RNAs and histone modifications, and functions in transposon
516 inactivation. *Plant Cell Physiol.* 53: 766-784.

517

518 Shao, Z.Q., Zhang, Y.M., Hang, Y.Y., Xue, J.Y., Zhou, G.C., Wu, P., et al. (2014) Long-term
519 evolution of nucleotide-binding site-leucine-rich repeat genes: understanding gained from and
520 beyond the legume family. *Plant Physiol.* 166: 217-234.

521

522 Simon, S.A. and Meyers, B.C. (2011) Small RNA-mediated epigenetic modifications in

523 plants. *Curr. Opin. Plant Biol.* 14: 148-155.

524

525 Takken, F.L. and Goverse, A. (2012) How to build a pathogen detector: structural basis of
526 NB-LRR function. *Curr. Opin. Plant Biol.* 15: 375-384.

527

528 Wei, W., Ba, Z., Gao, M., Wu, Y., Ma, Y., Amiard, S., et al. (2012) A role for small RNAs in
529 DNA double-strand break repair. *Cell* 149: 101-112.

530

531 Yan, S., Wang, W., Marques, J., Mohan, R., Saleh, A., Durrant, W.E., et al. (2013) Salicylic
532 acid activates DNA damage responses to potentiate plant immunity. *Mol. Cell* 52: 602-610.

533

534 Yang, Y.G. and Qi, Y. (2015) RNA-directed repair of DNA double-strand breaks. *DNA*
535 *Repair (Amst.)* 32: 82-85.

536

537 Yao, Y., Bilichak, A., Golubov, A. and Kovalchuk, I. (2011) Local infection with oilseed rape
538 mosaic virus promotes genetic rearrangements in systemic Arabidopsis tissue. *Mutat. Res.*
539 709-710: 7-14.

540

541 Yi, H. and Richards, E.J. (2007) A cluster of disease resistance genes in Arabidopsis is
542 coordinately regulated by transcriptional activation and RNA silencing. *Plant Cell* 19:
543 2929-2939.

544

545 Yi, H. and Richards, E.J. (2008) Phenotypic instability of Arabidopsis alleles affecting a

546 disease Resistance gene cluster. *BMC Plant Biol.* 8: 36.

547

548 Yi, H. and Richards, E.J. (2009) Gene duplication and hypermutation of the pathogen

549 Resistance gene SNC1 in the Arabidopsis bal variant. *Genetics* 183: 1227-1234.

550

551

552 **Figure Legends**

553

554 **Fig. 1**

555 Morphological reversion event are frequently observed in *uni-1D/+* plants.

556 (A) The original *uni-1D/+* (Ws) plant (left) and the *uni-1D/+* plant displaying morphological
557 reversion (right). The dotted circle indicates a morphologically reverted wild-type-like stem
558 that emerges from the *uni-1D/+* plant body. (B) Spontaneous mutations are indicated along
559 the UNI protein structure. CC, NB and LRR indicate coiled-coil, nucleotide-binding site and
560 leucine-rich repeat domains, respectively. The white circle indicates the original *uni-1D*
561 mutation site. Δ s indicate deletion mutations. (C) A *de novo* mutation that attenuates the
562 UNI-1D protein activity occurs within the *uni-1D* gene in one cell at a leaf axil where axillary
563 stems are generally formed. Then, the mutated cell, which is released from the growth defect
564 by *uni-1D*, eventually gives rise to a wild-type-like stem.

565

566 **Fig. 2**

567 EMS treatment significantly enhances the reversion frequency.

568 (A) Seeds were treated with indicated concentration of EMS. The rate of the individuals
569 displaying morphological reverted stems among the grown *uni-1D/+* population is shown as
570 solid circles and the solid line (the left Y-axis) and the germination rate is shown as open
571 circles and the dotted line (the right Y-axis). Data are means of three independent experiments
572 with error bars representing SD. Asterisks indicate significant differences by Student's *t* test
573 compared to mock conditions (*P value <0.05, **P value <0.01). (B) Induced mutations are
574 indicated along the UNI protein structure as shown in Fig. 1B.

575

576 **Fig. 3**

577 Effects of the original *uni-1D* gene structure and background on the reversion frequency.

578 (A) The gene structure around the *UNI* locus. Arrows indicate genes. The bar indicates the 5.3

579 kb fragment used to make *uni-1D^{T/+}* plants. (B) *uni-1D/+* (Ws), *uni-1D^{T/+}* (Ws) and *uni-1D/+*

580 (Col) seeds were treated with 0.3% EMS. The shown reversion rates are means of three

581 independent experiments with SD. Student's *t* test showed that no significant (n.s.) difference

582 was observed among the three conditions (P value >0.05).

583

584 **Fig. 4**

585 Effects of Zeocin- or HU-treatments on the reversion frequency and induced mutations.

586 (A) *uni-1D/+* plants were treated with Zeocin or HU. The shown reversion rates are means of

587 three independent experiments with SD. Asterisks indicate significant differences by Student's

588 *t* test compared to mock conditions (*P value <0.05, **P value <0.01). (B) Induced mutations

589 are indicated along the UNI protein structure as shown in Fig. 1B. The upper and lower sides

590 show Zeocin-induced deletions and HU-induced point mutations, respectively. Δ s mean

591 deletion mutations.

592

593 **Fig. 5**

594 Effects of inactivation of SA pathway on the reversion frequency.

595 *uni-1D/+* (Col) and *sid2 uni-1D/+* (Col) seeds were treated with 0.3% EMS. The shown

596 reversion rates are means of three independent experiments with SD. Asterisks indicate

597 significant differences by Student's *t* test (**P value <0.01).

598

599 **Fig. 6**

600 Effects of inactivation of DNA damage sensor pathway on the reversion frequency.

601 *uni-1D/+* (Ws), *atr uni-1D/+* (Ws) and *atm uni-1D/+* (Ws) were treated with 0.3% EMS. The

602 shown reversion rates are means of three independent experiments with SD. Asterisks

603 indicate significant differences by Student's *t* test (*P value <0.05, **P value <0.01).

604

605 **Fig. 7**

606 Spectrum of spontaneous *de novo* SNPs detected in wild type and *uni-1D^{T/+}*.

607 (A) Illustration of procedures in this assay. *De novo* SNPs were analyzed using 4 independent

608 lines per genotype, which were all derived from a single Col-0 individual. The Col-0 was

609 transformed with the *uni-1D* genomic fragment (Fig. 3A) to generate *uni-1D^{T/+}*. These lines

610 were maintained by selfing and single-seed descent during 5 generations, and then subjected

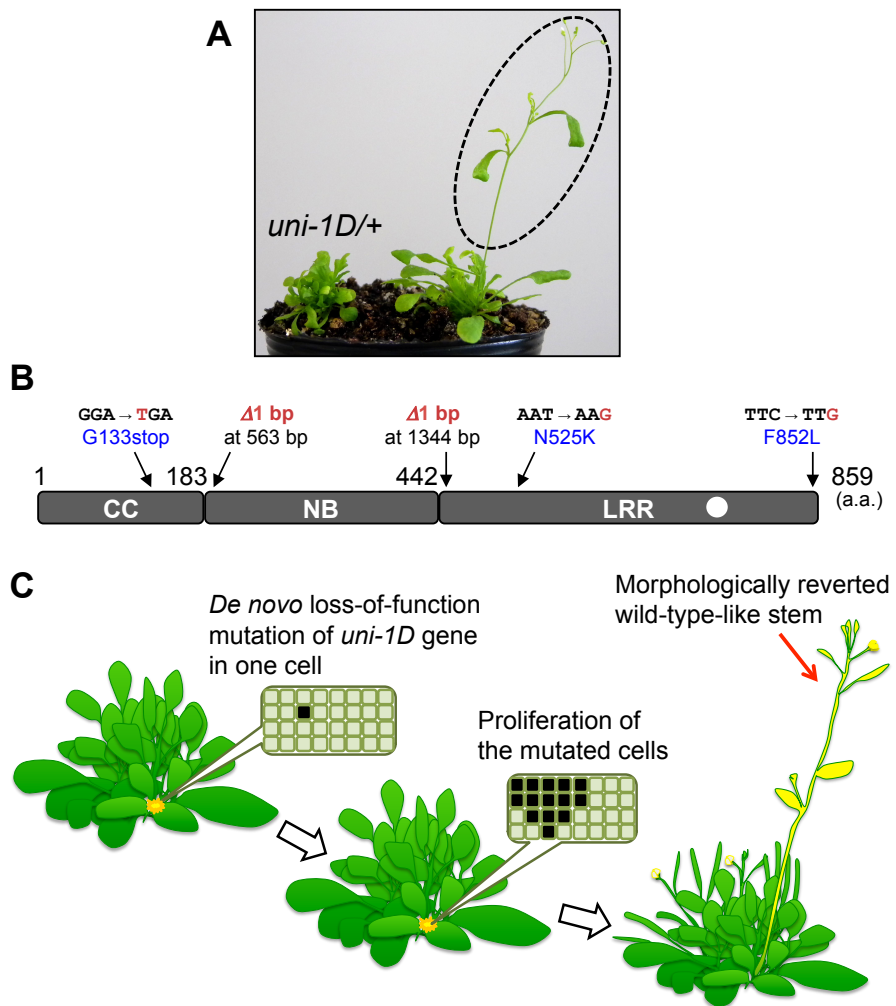
611 to genome sequencing. (B-C) (B) The number of detected *de novo* SNPs and their distribution

612 in chromosomes, (C) spectrum of nucleotide substitution types and (D) categorization of the

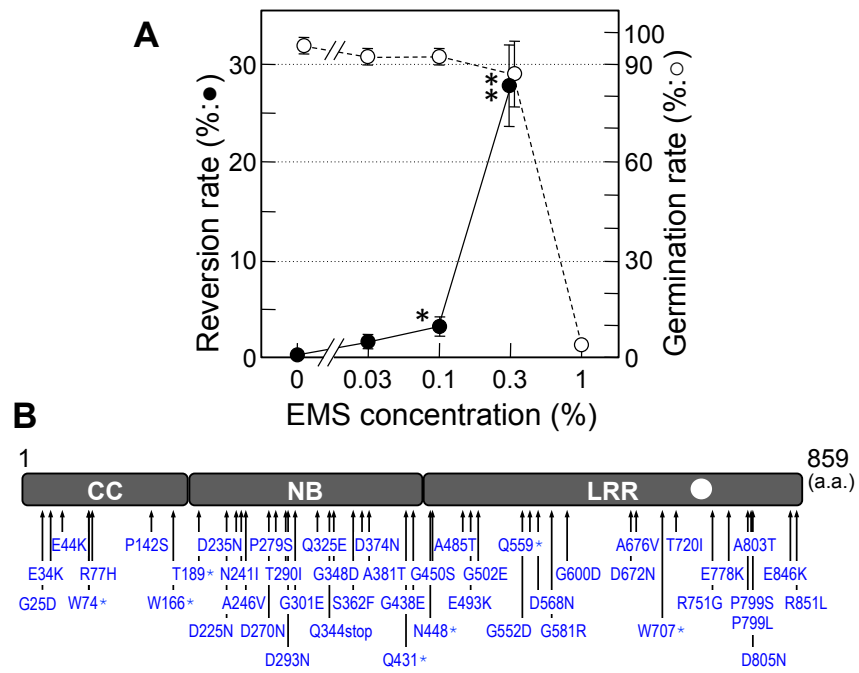
613 SNPs according to genic characters are shown. Four independent lines per genotype were

614 analyzed and data are means with error bars representing SD.

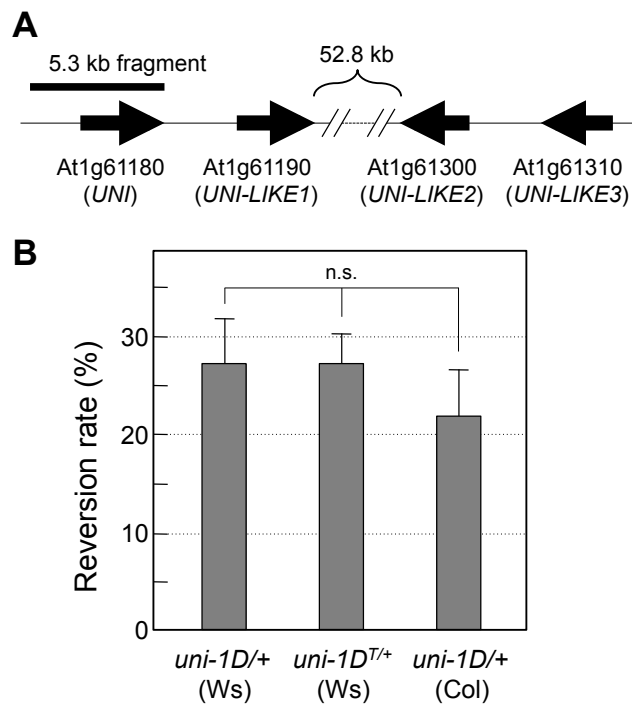
Ogawa et al. Fig. 1



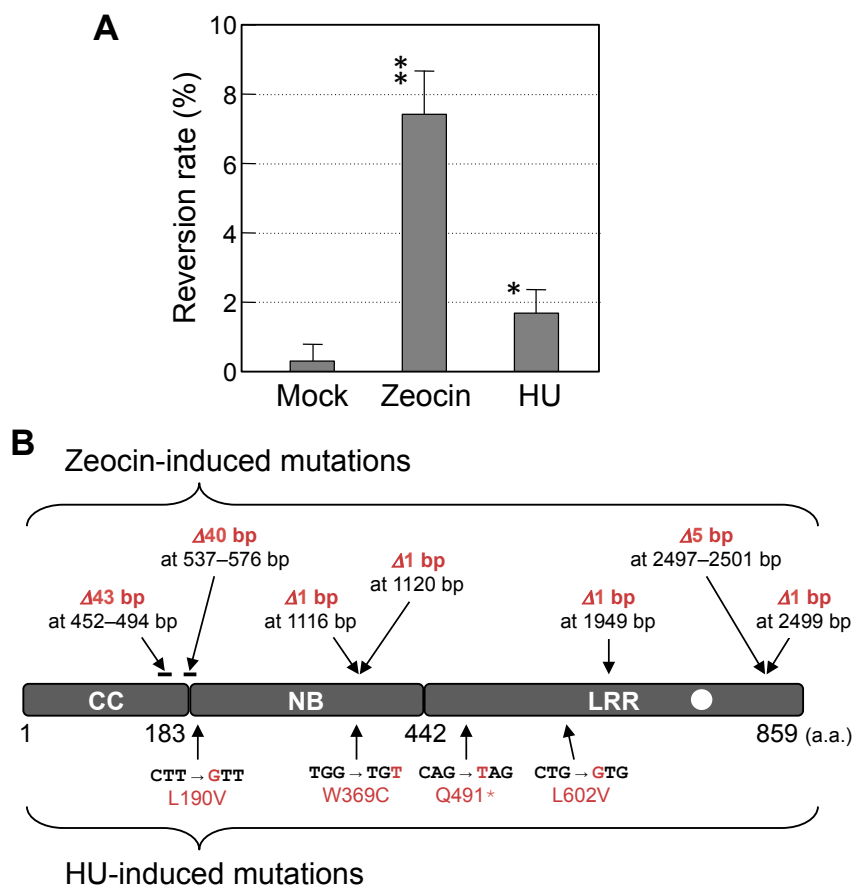
Ogawa et al. Fig. 2



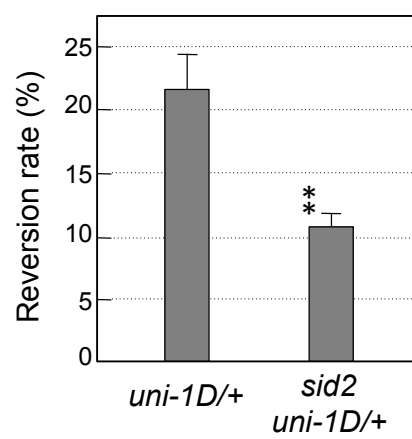
Ogawa et al. Fig. 3



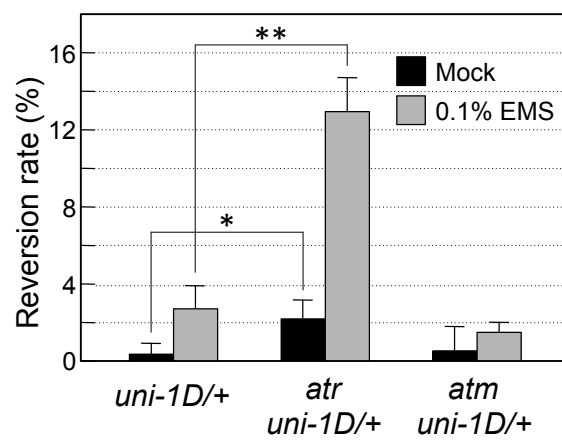
Ogawa et al. Fig. 4



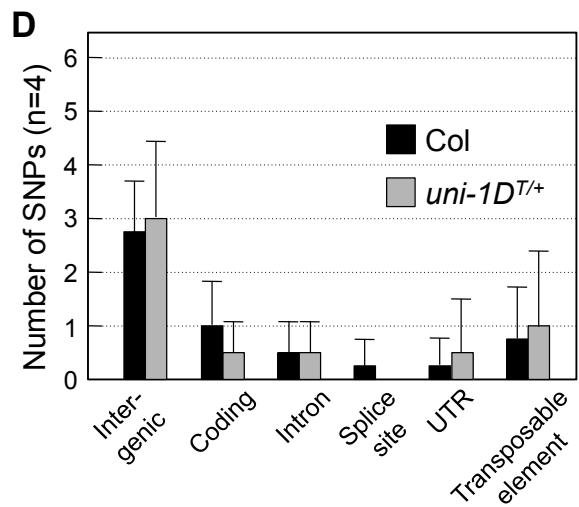
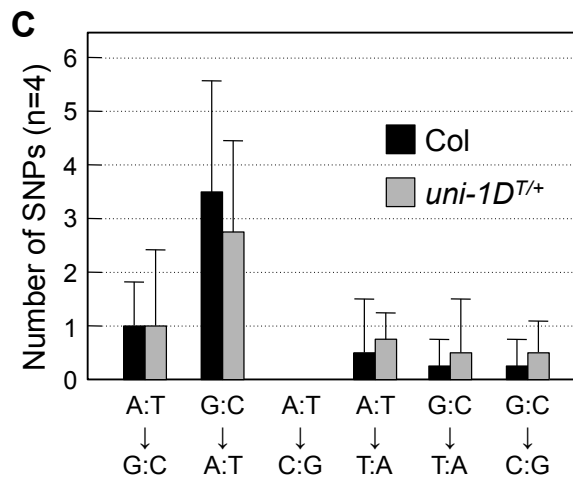
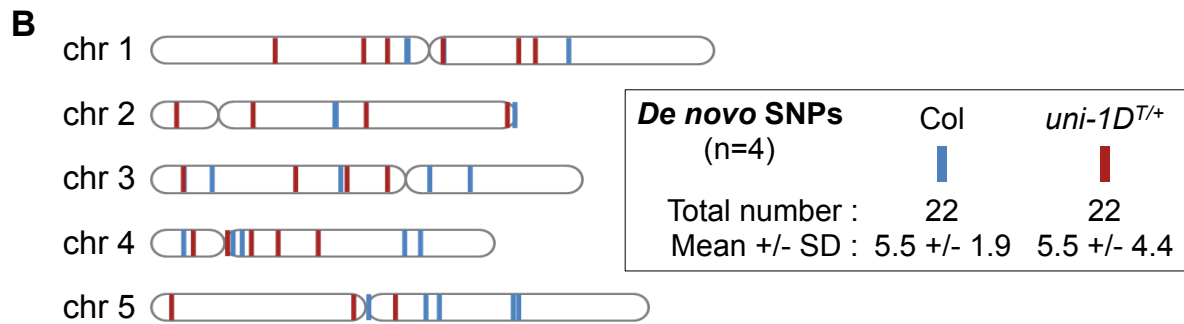
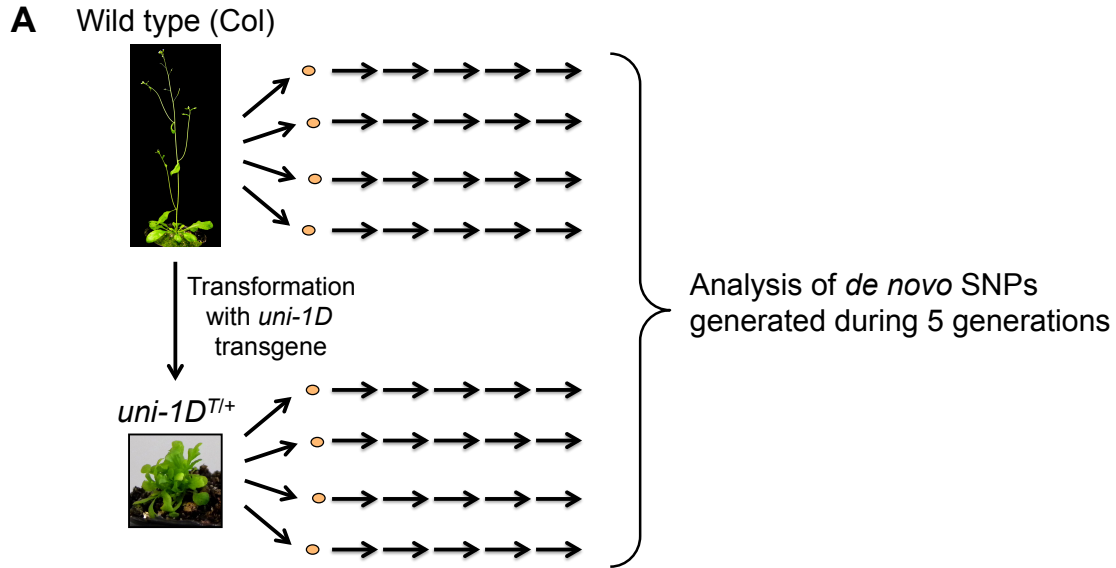
Ogawa et al. Fig. 5

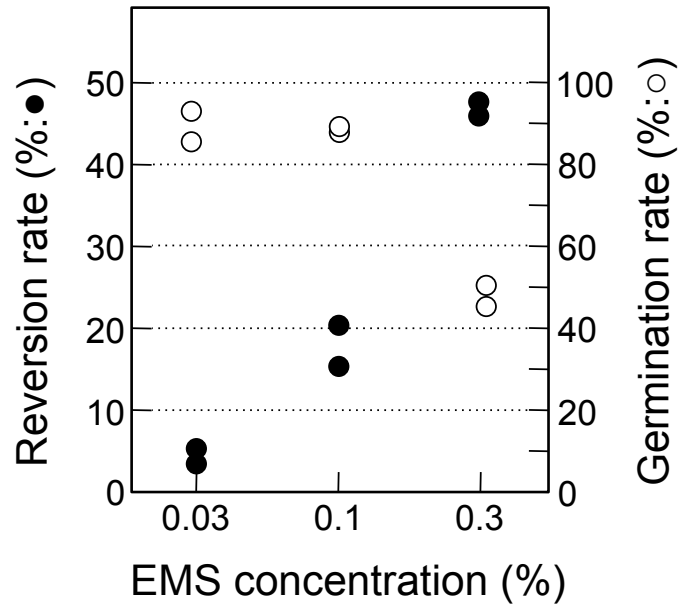


Ogawa et al. Fig. 6



Ogawa et al. Fig. 7





Supplementary Fig. 1

Effects of EMS treatment on frequency of morphological reversion and germination rate in *uni-1D/+*.

uni-1D/+ (Ws) seeds were treated with indicated concentrations of EMS for 27 hours. The reversion rates (solid circles, the left Y-axis) and germination rates (open circles, the right Y-axis) in two independent experiments are shown.

Supplementary Table 1

List of spontaneous *de novo* SNPs detected in wild type and *uni-ID^{T/+}*

Line	Chromosome	Position	Substitution	AGI code	Genic characters
Col #1	1	13534271	G→A	AT1G36160	CODING_NON_SYNONYMOUS
Col #1	1	22524457	A→T	AT1G61120	INTRONIC
Col #1	2	19542633	A→G	-	INTERGENIC
Col #1	3	1202319	A→G	AT3G04490	CODING_NON_SYNONYMOUS
Col #1	3	9885223	C→G	-	INTERGENIC
Col #1	4	3907807	G→T	-	INTERGENIC
Col #1	5	19438662	A→T	-	INTERGENIC
Col #2	1	13606099	C→T	-	INTERGENIC
Col #2	1	15603937	C→T	AT1G41830	CODING_SYNONYMOUS
Col #2	2	9630433	G→A	AT2G22660	3'UTR
Col #2	3	14815764	A→G	AT3G42717	TRANSPOSABLE_ELEMENT
Col #2	3	17061040	G→A	-	INTERGENIC
Col #2	4	4410106	G→A	AT4G07600	TRANSPOSABLE_ELEMENT
Col #2	5	14608961	C→T	-	INTERGENIC
Col #3	2	9561564	G→A	-	INTERGENIC
Col #3	4	13429719	G→A	AT4G26620	CODING_SYNONYMOUS
Col #3	5	15349385	C→T	-	INTERGENIC
Col #4	3	2742426	C→T	AT3G08980	INTRONIC
Col #4	4	1182344	A→G	AT4G02680	SPLICE_SITE
Col #4	4	14310986	C→T	-	INTERGENIC
Col #4	5	11426393	G→A	AT5G31572	TRANSPOSABLE_ELEMENT
Col #4	5	19740642	C→T	-	INTERGENIC
<i>uni-ID^{T/+}</i> #1	1	15548247	C→T	AT1G41790	TRANSPOSABLE_ELEMENT
<i>uni-ID^{T/+}</i> #1	1	20672868	C→T	-	INTERGENIC
<i>uni-ID^{T/+}</i> #1	2	19114681	G→A	-	INTERGENIC
<i>uni-ID^{T/+}</i> #1	5	12913310	T→A	-	INTERGENIC
<i>uni-ID^{T/+}</i> #2	1	11154709	C→T	-	INTERGENIC

<i>uni-ID^{T/+}</i> #2	2	5013067	C→G	-	INTERGENIC
<i>uni-ID^{T/+}</i> #3	1	19754140	A→G	-	INTERGENIC
<i>uni-ID^{T/+}</i> #3	3	7385964	A→T	-	INTERGENIC
<i>uni-ID^{T/+}</i> #3	3	10233797	C→T	AT3G27640	INTRONIC
<i>uni-ID^{T/+}</i> #3	4	6409241	C→T	AT4G10340	CODING_SYNONYMOUS
<i>uni-ID^{T/+}</i> #4	1	6235799	C→T	-	INTERGENIC
<i>uni-ID^{T/+}</i> #4	1	12485216	A→T	-	INTERGENIC
<i>uni-ID^{T/+}</i> #4	2	775183	A→G	AT2G02760	3'UTR
<i>uni-ID^{T/+}</i> #4	2	11287413	G→C	AT2G26540	3'UTR
<i>uni-ID^{T/+}</i> #4	3	1147306	A→G	AT3G04340	INTRONIC
<i>uni-ID^{T/+}</i> #4	3	12469255	G→A	AT3G30790	TRANSPOSABLE_ELEMENT
<i>uni-ID^{T/+}</i> #4	4	1704227	C→T	-	INTERGENIC
<i>uni-ID^{T/+}</i> #4	4	3608656	G→T	AT4G06589	TRANSPOSABLE_ELEMENT
<i>uni-ID^{T/+}</i> #4	4	4921559	G→A	AT4G08056	TRANSPOSABLE_ELEMENT
<i>uni-ID^{T/+}</i> #4	4	8626372	G→T	AT4G15100	CODING_SYNONYMOUS
<i>uni-ID^{T/+}</i> #4	5	503277	C→T	-	INTERGENIC